

On Xenon Fission Product Poisoning

Barry Ganapol, Sebastian Schunert,
Frederick N Gleicher, Richard C
Martineau, Mark D DeHart

September 2019



The INL is a U.S. Department of Energy National Laboratory
operated by Battelle Energy Alliance

On Xenon Fission Product Poisoning

**Barry Ganapol, Sebastian Schunert, Frederick N Gleicher, Richard C Martineau,
Mark D DeHart**

September 2019

**Idaho National Laboratory
Idaho Falls, Idaho 83415**

<http://www.inl.gov>

**Prepared for the
U.S. Department of Energy
Under DOE Idaho Operations Office
Contract DE-AC07-05ID14517**

Investigation of Xenon Oscillations via Point Kinetics

B. Ganapol

Department of Aerospace and Mechanical Engineering, University of Arizona: 1130 N. Mountain Ave., Tucson, AZ, 85721,
Ganapol@cowboy.ame.arizona.edu

S. Schunert, F. Gleicher, and R. Martineau
 Idaho National Laboratory, Idaho Falls, Idaho

INTRODUCTION

We all appreciate the special role Xenon-135 plays in reactor transients. Unless there is sufficient reactivity override, on shutdown a conventional reactor cannot immediately restart because of the buildup of strongly absorbing Xenon from Iodine decay and the absence of neutron flux to continue its elimination. We are also aware of how the flux imbalance in a large reactor core gives rise to Xenon induced power precession around the core in unpredictable ways. In addition, with regard to computational methods, we lack readily accessible numerical algorithms enabling reliable characterization of Xenon oscillations with simple models to explain this fundamentally important phenomenon. Nowhere is this more apparent than in the classroom. In this presentation, we first consider a new 12-element comprehensive decay to model Xenon and its corresponding numerical implementation and verification to establish a predictive model of Xenon buildup in a constant flux. We then follow with a reduced self-consistent flux model in an infinite reactor- a model not found in textbooks. This presentation should appeal to those interested in developing high order numerical methods for reactor transients.

XENON BUILDUP IN A CONSTANT FLUX

We begin with Xe building up from the startup of a reactor from zero power. Figure 1 shows the entire decay scheme to Xe-135 (12) from Indium-135 (1) and the isotopic ID numbers (in parenthesis) used in the analysis to follow. The analysis found in textbooks assumes all isotope production from fission prior to Iodine-135 (10) is accounted for in the Iodine yield, where the analysis usually begins. In addition, $^{135}\text{Xe}^m$ (11) is ignored. We consider all isotopes in our startup model and assume a constant flux for the initial development of the numerical algorithm.

The fundamental decay equations, in vector form, are

$$\frac{dy(t)}{dt} = Ay(t) + S(t), \quad (1a)$$

$$y(t) \equiv [y_1 \ y_2 \ \dots \ y_{12}]^T \quad (1b,c)$$

$$S(t) \equiv [\gamma_1 \Sigma_f \phi \ \gamma_2 \Sigma_f \phi \ \dots \ \gamma_{12} \Sigma_f \phi]^T$$

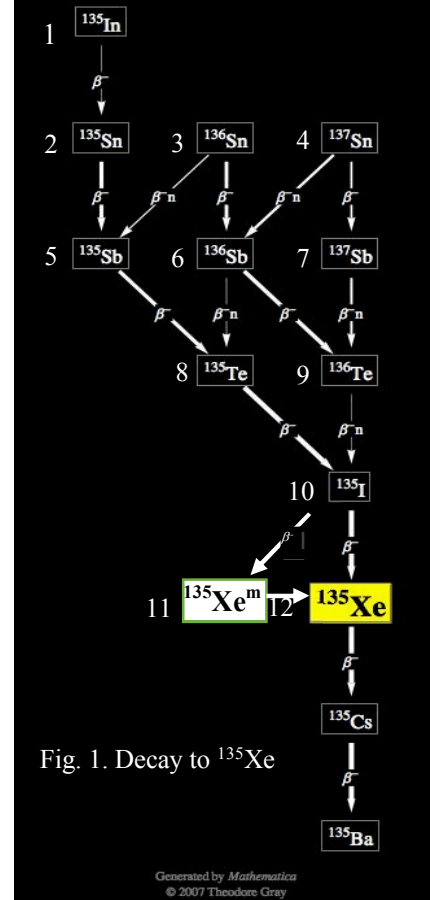


Fig. 1. Decay to ^{135}Xe

and the non-zero elements of the Jacobian matrix A are

$$\begin{aligned} a(1,1) &= (\lambda_1 + \sigma_1 \phi) & a(5,3) &= \beta_3 \lambda_3 \\ a(2,1) &= \lambda_1 & a(5,5) &= \lambda_5 + \sigma_5 \phi \\ a(2,2) &= (\lambda_2 + \sigma_2 \phi) & a(6,3) &= (1 - \beta_3) \lambda_3 \\ a(3,3) &= (\lambda_3 + \sigma_3 \phi) & a(6,4) &= \beta_4 \lambda_4 \\ a(4,4) &= (\lambda_4 + \sigma_4 \phi) & a(6,6) &= \lambda_6 + \sigma_6 \phi \\ a(7,4) &= (1 - \beta_4) \lambda_4 & a(9,6) &= (1 - \beta_6) \lambda_6 \\ a(7,7) &= \lambda_7 + \sigma_7 \phi & a(9,7) &= \lambda_7 \\ a(8,5) &= \lambda_5 & a(9,9) &= \lambda_9 + \sigma_9 \phi \\ a(8,6) &= \beta_6 \lambda_6 & a(10,8) &= \lambda_8 \\ a(8,8) &= \lambda_8 + \sigma_8 \phi & a(10,9) &= \lambda_9 \end{aligned}$$

$$\begin{aligned}
a(10,10) &= \lambda_8 + \sigma_8 \phi \\
a(11,10) &= \beta_{10} \lambda_{10} \\
a(11,11) &= \lambda_{11} + \sigma_{11} \phi \\
a(12,10) &= (1 - \beta_{10}) \lambda_{10} \\
a(12,11) &= \lambda_{11} \\
a(12,1) &= \lambda_{12} + \sigma_{12} \phi
\end{aligned}$$

The decay constants (λ_i), absorption cross sections (σ_i), yields (γ) and branching ratios (β_i) are given in Table 1; ϕ is the constant flux. Note that the absorption cross sections for elements before Iodine are not available and were therefore assumed zero.

Essentially, one applies the most fundamental of implicit numerical schemes to solve Eqs(1), *i.e.*, Backward Euler Finite Difference BEFD as presented previously¹. The algorithm begins by assuming the backward finite difference approximation for the derivative to give

$$y_j = [I - hA]^{-1} [y_{j-1} + hS_j], j = 1, \dots, n, \quad (2)$$

with zero initial condition $y_0 = 0$. Note that the time interval has been discretized over the desired time edit t_e such that $h = t_e/n$, where h is the uniform interval. The novelty of the proposed solution is inclusion of convergence acceleration over discretization h through Richardsons acceleration² by varying n .

For a constant flux of $10^{14}n/cm^2\cdot s$, Fig. 2a shows the isotope traces for a clean core reactor startup. The evolution of the 12 elements including Xenon is as expected. In particular, the evolution of the preceding five isotopes to Xe, emphasized in gray, dominate at equilibrium.

Table 1. Isotopic Data.

#	Symbol	$T_{1/2}$	σ_a^*	Yield(γ)	Branching Ratio
1	¹³⁵ In	0.092s	0	7.256e-11	0
2	¹³⁵ Sn	0.53s	0	6.270e-06	0
3	¹³⁶ Sn	0.25s	0	1.5699e-07	0.7
4	¹³⁷ Sn	0.19s	0	1.86e-07	0.42
5	¹³⁵ Sb	1.74s	0	1.4514e-03	0
6	¹³⁶ Sb	0.923s	0	1.1490e-04	0.923
7	¹³⁷ Sb	0.45s	0	7.4333e-06	0
8	¹³⁵ Te	19s	0	3.2162e-02	0
9	¹³⁶ Te	17.5s	0	1.3174e-02	0
10	¹³⁵ I	6.57hr	7.0b	2.9274e-02	0.8349
11	¹³⁵ Xe ^m	15.3m	3.5e06b	1.8145e-03	0
12	¹³⁶ Xe	9.14hr	3.5e06b	7.5196e-04	0

* Zeros entered when no data available

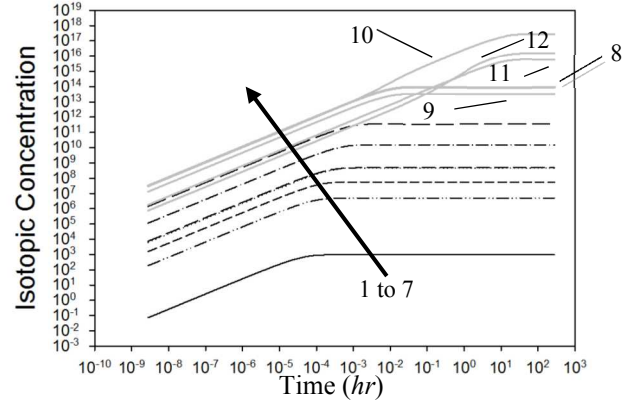


Fig. 2a. Isotopic Traces to Xe and I equilibrium.

Actually, the concentrations are divided by the total fission cross section Σ_f since it factors out of the evolution equations. The dominance of the two isotopes of Te, I and Xe is more easily seen in Fig. 2b, which gives the asymptotic isotopic traces relative to the asymptotic concentrations of Table 2. Note that isotopes 10 (I) and 11 (Xe^m) are indistinguishable. Thus, all isotopes except the last three come to their asymptotic equilibrium within 100s of startup. This justifies considering only I and Xe in Xenon poisoning analyses as is normally done.

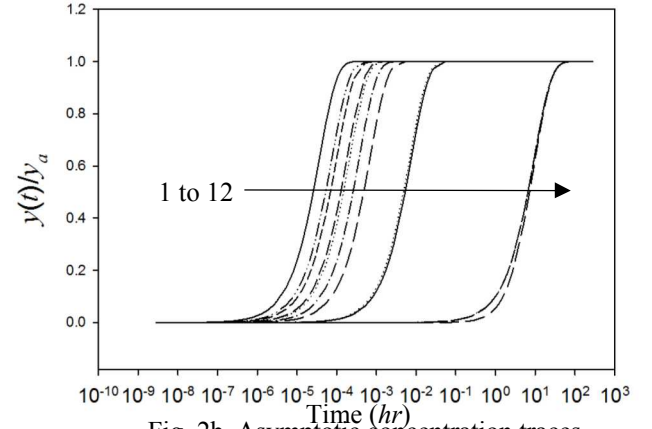


Fig. 2b. Asymptotic concentration traces.

To end this demonstration, we show the advantage of Richardsons extrapolation. It is no secret that a finite difference numerical algorithm is not required for this case since the Jacobian matrix is constant in time. One can simply diagonalize matrix A and the solution to Eqs(1) is

$$y(t) = Te^{\lambda t}T^{-1}y(0) + T[I - e^{\lambda t}]\lambda^{-1}T^{-1}S, \quad (3)$$

where T is the matrix of eigenvectors and λ is a diagonal matrix of eigenvalues. With an analytical solution, one can then find the exact relative error of the BEFD algorithm.

TABLE 2. Asymptotic Isotopic Concentrations y_a .

#	$(\omega_j \equiv \lambda_j + \sigma_j \phi)$
1	$\gamma_1 \Sigma_f \phi / \omega_1$
2	$(\lambda_1 y_{1a} + \gamma_2 \Sigma_f \phi) / \omega_2$
3	$\gamma_3 \Sigma_f \phi / \omega_3$
4	$\gamma_4 \Sigma_f \phi / \omega_4$
5	$(\beta_3 \lambda_3 y_{3a} + \gamma_5 \Sigma_f \phi) / \omega_5$
6	$(\beta_4 \lambda_4 y_{4a} + (1 - \beta_3) \lambda_3 y_{3a} + \gamma_6 \Sigma_f \phi) / \omega_6$
7	$((1 - \beta_4) \lambda_4 y_{4a} + \gamma_7 \Sigma_f \phi) / \omega_7$
8	$(\beta_6 \lambda_6 y_{6a} + \lambda_5 y_{5a} + \gamma_8 \Sigma_f \phi) / \omega_8$
9	$((1 - \beta_6) \lambda_6 y_{6a} + \lambda_7 y_{7a} + \gamma_9 \Sigma_f \phi) / \omega_9$
10	$(\lambda_8 y_{8a} + \lambda_9 y_{9a} + \gamma_{10} \Sigma_f \phi) / \omega_{10}$
11	$(\beta_{10} \lambda_{10} y_{10a} + \gamma_{11} \Sigma_f \phi) / \omega_{11}$
12	$((1 - \beta_{10}) \lambda_{10} y_{10a} + \lambda_{11} y_{11a} + \gamma_{12} \Sigma_f \phi) / \omega_{12}$

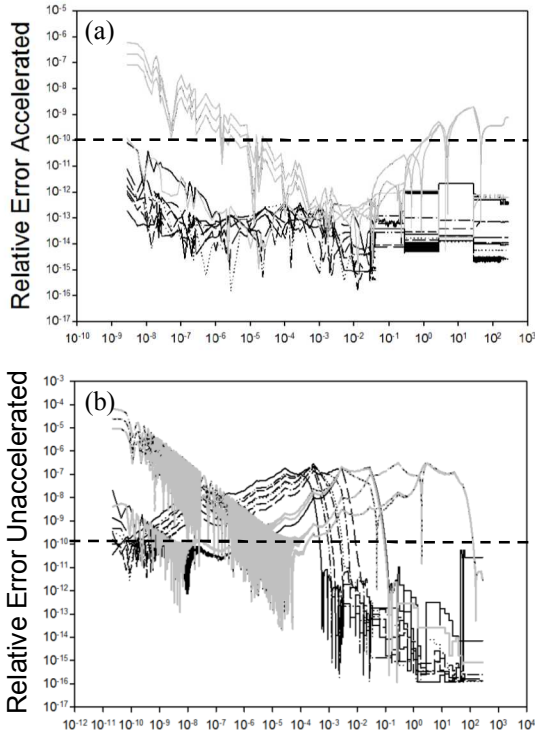


Fig. 3a,b. Exact relative errors for accelerated and unaccelerated approximations.

Figures 3a,b give the relative error for the accelerated and unaccelerated solutions. The unaccelerated solution is just the converged BEFD algorithm at subsequently halved time steps; while, Richardson's extrapolation spawns a new FD scheme for each halved interval grid over an edit. The relative errors for the last four isotopic concentrations are in gray. One can readily observe, from the line at 10^{-10}

relative error, the advantage of the accelerated solution by orders of magnitude.

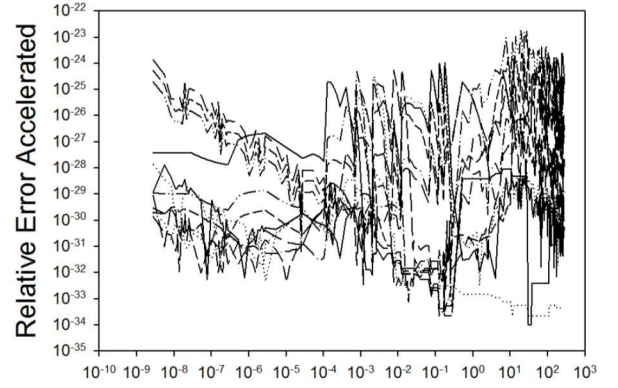


Fig. 4. All traces with extreme (QP) accuracy.

As a final result, we find the solution in Quadruple Precision (QP) in Fig. 4 to an extreme accuracy of 10^{-24} . This case is included to demonstrate, counter to what we learned in our elementary numerical methods class, one can make simple finite difference algorithms exceptionally accurate.

XENON BUILDUP IN A SELF-CONSISTENT FLUX

The case for Xenon buildup in a self-consistent flux, where the variation of Iodine and Xenon influence the flux itself, presents special modelling and numerical challenges. The initial challenge is to decide on the flux model that incorporates the temporal change in Iodine and Xenon concentrations with the flux variation. The simplest and most easily understood model is to couple the rate equations with the point kinetics equation describing integrated transient reactor behavior.

Hence, the point kinetics equations for the neutron flux ϕ and precursor concentrations C_l for six delayed groups

$$\frac{d\phi(t)}{dt} = \left[\frac{\rho(X(t)) - \beta}{\Lambda} \right] \phi(t) + \sum_{l=1}^6 \lambda_l C_l(t) \quad (4a,b)$$

$$\frac{dC_l(t)}{dt} = \frac{\beta_l}{\Lambda} \phi(t) - \lambda_l C_l(t), \quad l = 1, \dots, 6,$$

are coupled to the two rate equations

$$\begin{aligned} \frac{dI(t)}{dt} &= -(\lambda_I + \sigma_I \phi(I, X)) I(t) + \gamma_I \Sigma_f \phi(t) \\ \frac{dX(t)}{dt} &= -(\lambda_X + \sigma_X \phi(I, X)) X(t) + \\ &\quad + \lambda_I(t) I(t) + \gamma_X \Sigma_f \phi(t) \end{aligned} \quad (4c,d)$$

for Iodine (I) and Xenon (X) buildup. Only the last two equations of the previous Xe model are considered for simplicity and since they have been shown to be the most essential.

These equations connect through reactivity

$$\rho(X(t)) \approx \rho_0 - \frac{\sigma_X}{\Sigma_f} \left[\frac{\Sigma_f}{\Sigma_U} \right] [X(t) - X(0)],$$

where for ^{235}U fuel

$$\frac{\Sigma_f}{\Sigma_U} \approx 0.84.$$

The first term is an applied step change in reactivity, say from a control rod. The second arises from the imbalance of Xenon concentration as the flux level changes and accounts for the reactivity of the equilibrium Xenon compensated by the control rod of the initially critical reactor.

In an algebraic representation therefore, we are to solve

$$\frac{dy(t)}{dt} = A(I, X) y(t) + S(t) \quad (6a)$$

where

$$y(t) \equiv [\phi(t) \ C_1(t) \ \dots \ C_6(t) \ I(t) \ X(t)]^T \quad (6b)$$

with

$$A(I, X) \equiv \begin{bmatrix} (\rho(I, X) - \beta)/\Lambda & \lambda_1 & \dots & \lambda_6 & 0 & 0 \\ \frac{\beta_1}{\Lambda} & -\lambda_1 & 0 & \dots & \dots & \dots \\ \frac{\beta_2}{\Lambda} & 0 & \dots & \dots & \dots & \dots \\ \dots & \dots & \dots & \dots & \dots & \dots \\ \frac{\beta_6}{\Lambda} & 0 & \dots & 0 & -\lambda_6 & 0 \\ 0 & 0 & \dots & 0 & -(\lambda_I + \sigma_I \phi(t)) & 0 \\ 0 & \dots & \dots & 0 & \lambda_X & -(\lambda_X + \sigma_X \phi(t)) \end{bmatrix} \quad (6c)$$

Reactivity, inserted into an initially critical reactor at flux $\phi(0)$, where the Iodine and Xenon are in equilibrium as are the precursors, gives the initial conditions

$$\begin{aligned} C_l(0) &= \frac{\beta_l}{\lambda_l \Lambda} \phi(0), \quad l=1, \dots, 6 \\ I(0) &= \frac{\gamma_I \Sigma_f \phi(0)}{\lambda_I + \sigma_I \phi(0)} \\ X(0) &= \frac{\gamma_X \Sigma_f I(0) + \gamma_X \Sigma_f \phi(0)}{\lambda_X + \sigma_X \phi(0)}. \end{aligned} \quad (6d)$$

Since the Jacobian now depends on a changing flux, which itself depends on the isotopic concentrations, we must performed iteration. One does this through a fixed-point iteration updating the Jacobian matrix Eq(6c) at each iterate.

Figure 5a gives the flux transient starting at $10^7 \text{ n/cm}^2\text{-s}$ for increasing reactivity insertions. As one observes, with an insertion of only 0.0005\$ the Xenon and Iodine traces begin to oscillate. This, of course, is the classical result that comes with an increasing flux leading to higher Iodine concentration and increasing Xenon production lowering the flux, which decreases Xenon production from Iodine leading to a higher flux and more Iodine, and so on.... The corresponding I and Xe traces also oscillate as shown in Fig. 5b.

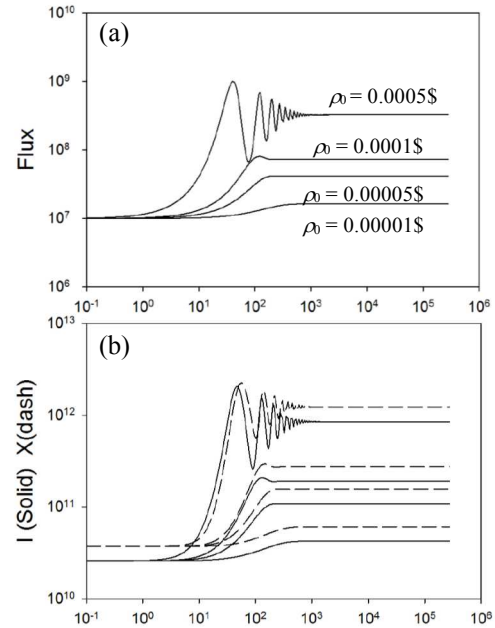


Fig.5 (a) Flux trace, (b) I and X traces

CONCLUSION

A simple flux coupled Iodine/Xenon model has been developed to demonstrate Xenon oscillations in an infinite reactor described by point kinetics. A future calculation will consider the full 12-isotope model with flux variation.

REFERENCES

1. B. Ganapol, et. al., A Backward Euler Doubling Feasibility Study Based on the Thorium Series Cascade, Las Vegas, American Nuclear Society National Meeting, 2016.
2. A. Sidi, *Practical Extrapolations Methods*, Cambridge University Press, Cambridge, 2003.
3. S. Glasstone and M. Edlund, *Elements of Nuclear Reactor Theory*, Van Nostrand Co., Inc. NY, 1952.